

• Supplementary file •

# Neuromorphic Terahertz Imaging Based on Carbon Nanotube Circuits

Nan YANG<sup>1,2†</sup>, Zhizhong SI<sup>1†</sup>,  
Xinhe WANG<sup>1,3\*</sup>, Xiaoyang LIN<sup>1,3\*</sup> & Weisheng ZHAO<sup>1,3</sup>

<sup>1</sup>School of Integrated Circuit Science and Engineering, Beihang University, Beijing 100191, China;

<sup>2</sup>

<sup>3</sup>Fert Beijing Institute, MIT Key Laboratory of Spintronics, School of Integrated Circuit Science and Engineering, Beihang University, Beijing 100191, China

## Appendix A: Simulation and experiment comparison of CNTs

In order to show that the simulation and the experiments in the reference has the consistent data, the parameters under different experimental conditions are simulated (Fig.1). We simulate the response strength of the carbon nanotube sensor under different THz irradiation intensity. The CNTs sensor layer consists of p-n junctions connected by source and drain electrodes. Focused illumination causes local heating of the p-n junction and thus a temperature difference between the p-n junction and the contacts. As a consequence, a voltage  $\Delta V$  is generated across the device due to the thermoelectric effect,  $\Delta V = S_p \Delta T_p - S_n \Delta T_n = (S_p - S_n) \Delta T$ , where  $S_p$  ( $S_n$ ) is the Seebeck coefficient of the p-type (n-type) portion of the CNTs [1]. So the corresponding response voltage or current are generated. The current-voltage characteristics of our CNTs sensing and its response to THz irradiation at 1.4 and 39 THz are shown in Fig. 1 (a) and (b), with the corresponding experimental reference data [1]. Fig.1 (c) and (d) show the power dependence of the photocurrent under illumination by a 375 nm and 808 nm laser in the simulation and experimental reference [2]. It can be observed that the photocurrent increases as the light intensity increases, which can be attributed to the photogenerated charge carrier efficiency is proportional to the absorbed photon flux. The simulation diameter range of carbon nanotubes is 0.8 nm-2.7 nm, and the result data is the optimal value of the simulation results. Compared with the experimental data in the same environment, there are some small differences, but they're similar. To sum up, it can be regarded as the simulation of CNTs as the sensing layer material in our system is feasible and has experimental reference basis.

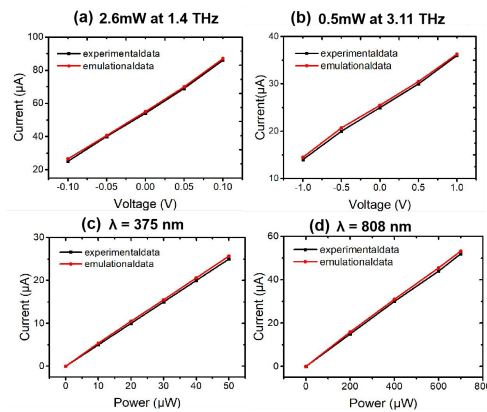


**Fig. 1** Responses of CNT detectors to electromagnetic signals: comparison of emulational and experimental data. (a)-(b) Current versus voltage for THz irradiation at 1.4 and 3.11 THz, respectively. The red lines are simulated results while the black lines are experimental references which from a flexible CNT-array-based THz scanner at room temperature [1]. (c)-(d) The responsivity of the photocurrent vs absorbed light power with wavelength 375nm and 808nm, respectively. The pink lines are simulated results and the blue lines are experimental references from [2]. In simulation, the diameters of CNTs are adopted within a reasonable range from 0.8 nm to 2.7 nm, and the result data is the optimal value.

<sup>1†</sup> These authors contribute equally

\*Corresponding authors (e-mails: xinhe@buaa.edu.cn and XYLin@buaa.edu.cn)

## Appendix B: Performance analysis of terahertz detection materials

As a simulated material with experimental reference data in the system of sensing layer, CNTs can detect terahertz range from 0.14 to 39 THz compared with other materials in Table 1 [3]. It has responsivity as high as  $\sim 2.5$  V/W and polarization ratio as high as  $\sim 5:1$  [3]. With the development of nanometer technology, the preparation technology of CNTs will be improved continually, which is expected to achieve a higher performance of responsiveness.

**Table 1** Comparison of Characterization Parameters of Different Materials Detected by Terahertz

materials	CNTs [4],[5],[3],[2]	CMOS [6]	GaN/AlGaIn [4]	Graphene [7]	GaAs/AlGaAs [5]
Responsivity	0.58 A/W (2.5 V/W)	$3.3 \times 10^3$ V/W	$48 \times 10^{-3}$ A/W	$45 \times 10^{-3}$ A/W	$6 \times 10^2$ V/W
NEP ( $\times 10^{-11}$ W/ $\sqrt{\text{Hz}}$ )	3.1	10.6	5.7	4.8	1000
Detection zone (THz)	0.14~39	0.3~3	0.1~1.8	0.4~2.2	0.235~0.24

According to the waveform analysis in Figure 1 (d) of the text, signals of three types of different images can be distinguished within one hundred nanoseconds. Therefore, it can be concluded that our system can monitor 10 million different signals within one second.

### References

- 1 D. Suzuki, S. Oda, and Y. Kawano, "A flexible and wearable terahertz scanner," *Nat. Photonics*, vol. 10, no. 12, pp. 809–813, 2016, doi: 10.1038/nphoton.2016.20930.
- 2 Y. Liu et al., "High-Performance, Ultra-Broadband, Ultraviolet to Terahertz Photodetectors Based on Suspended Carbon Nanotube Films," *ACS Appl. Mater. Interfaces*, vol. 10, no. 42, pp. 36304–36311, 2018, doi: 10.1021/acsami.8b14386.36
- 3 X. He et al., "Carbon nanotube terahertz detector," *Nano Lett.*, vol. 14, no. 7, pp. 3953 – 3958, 2014, doi: 10.1021/nl5012678.25
- 4 M. Bauer et al., "High-sensitivity wideband THz detectors based on GaN HEMTs with integrated bow-tie antennas," *Eur. Microw. Week 2015*, pp. 1–4, 2015, doi: 10.1109/EuMIC.2015.734505315.
- 5 G. C. Dyer, G. R. Aizin, J. L. Reno, E. A. Shaner, and S. J. Allen, "Novel tunable millimeter-wave grating-gated plasmonic detectors," *IEEE J. Sel. Top. Quantum Electron.*, vol. 17, no. 1, pp. 85–91, 2011, doi: 10.1109/JSTQE.2010.204909616.
- 6 Z. Y. Liu, L. Y. Liu, J. Yang, and N. J. Wu, "A CMOS Fully Integrated 860-GHz Terahertz Sensor," *IEEE Trans. Terahertz Sci. Technol.*, vol. 7, no. 4, pp. 455–465, 2017, doi: 10.1109/TTHZ.2017.269204017.
- 7 K. Ikamas, D. Cibiraite, A. Lisauskas, M. Bauer, V. Krozer, and H. G. Roskos, "Broadband Terahertz Power Detectors Based on 90-nm Silicon CMOS Transistors with Flat Responsivity Up to 2.2 THz," *IEEE Electron Device Lett.*, vol. 39, no. 9, pp. 1413–1416, 2018, doi: 10.1109/LED.2018.2859300.38